UPPSALA
UNIVERSITET

Hemagglutinin reassortment dynamics of the zoonotic H9N2 avian influenza virus

Steinar S Mannsverk

Master Degree Project in Infection Biology, 45 credits.
Spring 2021

Department: IMBIM, Uppsala University
Supervisor: Mahmoud Naguib
Co-supervisor: Patrik Ellström

Table of Contents

ABSTRACT

The H9N2 avian influenza virus (AIV) has emerged, spread and established itself in poultry globally, in just under 30 years. During this time, multiple reassortants of H9N2 with increased zoonotic potential have been isolated in poultry and humans, causing a major threat to the economy and global health. Curiously, H9N2 appears to be compatible with multiple Hemagglutinin (HA) and Neuraminidase subtypes, in nature. Here, the aim was to investigate the HA reassortment dynamics of the poultry adapted H9N2 AIV, in a laboratory setting. Firstly, HA subtypes from wild bird isolates were cloned, before being co-transfected with the backbone of a chicken H9N2 AIV. The rescued H9N2 reassortants were titred on cells before the replication kinetics of a subset of the HA reassortants was assessed. The cDNA sequence of seven HA subtypes induced extensive recombination in *E. coli*, but ultimately ten out of eleven available HA subtypes were successfully cloned. Further, the chicken H9N2 AIV was compatible with all ten HA subtypes, producing infectious viral particles after co-transfection. However, all HA reassortants displayed decreased replicative fitness in MDCK-2 cells, compared to the wild-type virus. Interestingly, HA subtypes with similar genotypes cluster into distinct HA clades and groups, but these HA clades did not correlate with the replicative fitness of the reassortants. This study suggests that poultry adapted H9N2 AIV is compatible with many HA subtypes, highlighting the importance of reducing its spread in poultry, to reduce reassortment opportunities.

POPULAR SUMMARY

Could the H9N2 avian influenza virus cause the next pandemic?

Besides causing the common "seasonal flu", influenza viruses occasionally cause global pandemics. In fact, since 1900 there have been five pandemics caused by influenza viruses, including the 1918 "Spanish Flu" which is the deadliest event in recorded human history. But to many people's surprise, pandemics are not caused by human seasonal influenza viruses. Almost all influenza virus pandemics originate from avian influenza viruses (also known as "bird flu") and as the name suggests, they come from birds.

The first step towards a pandemic involves an avian influenza virus from wild birds infecting domesticated farm animals. Circulation of the virus in farm animals increases the likelihood of contact with humans and gives the virus ample opportunity to adapt. Worryingly, this is exactly what has seemed to happen with the H9N2 avian influenza virus. An outbreak of H9N2 in China in the early 1990's spread among poultry to the majority of Asia, the Middle East and North and West Africa. Since then, H9N2 has infected humans and given rise to multiple new virus variants, posing a major risk to global health and the economy.

The immune response to influenza viruses is directed against its surface proteins, mainly Hemagglutinin. Currently, sixteen subtypes (or variants) of the Hemagglutinin protein have been characterized in avian influenza viruses. Moreover, the human population has only been exposed to three subtypes, leaving us without immunity to the remaining thirteen Hemagglutinin subtypes. As its genome consists of eight separate gene segments, influenza viruses have the unique ability to exchange gene segments with each other (see picture below: **Reassortment**). This process is named reassortment and is implicated in most influenza virus pandemics.

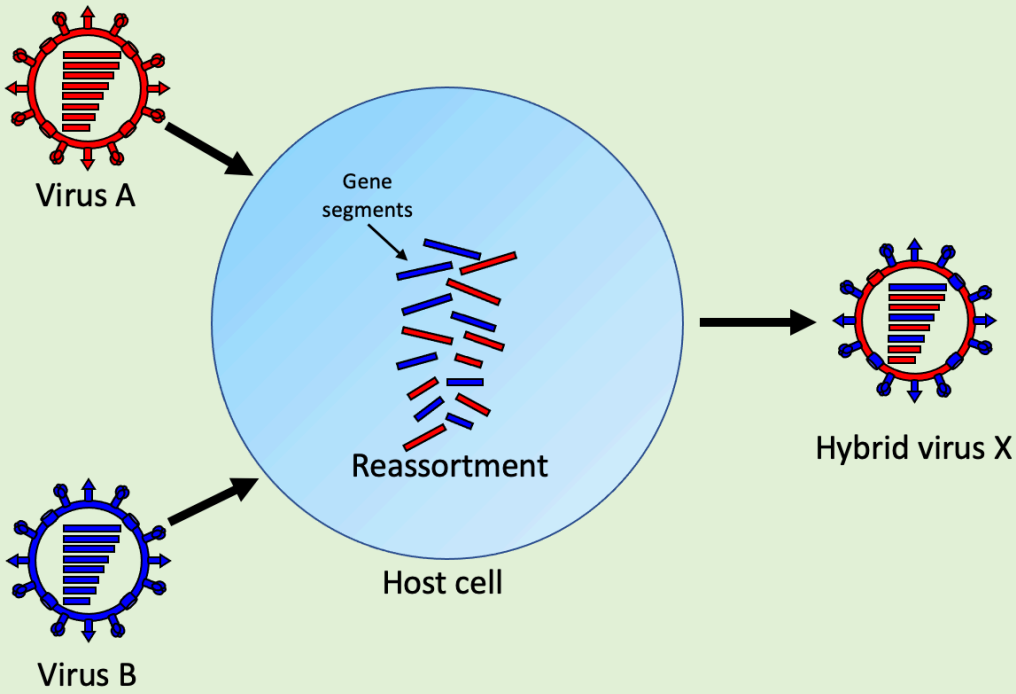

Reassortment: when two different influenza viruses infect the same host and cell simultaneously, their gene segments can mix to create a new hybrid virus carrying gene segments from both viruses.

Reassortment between H9N2 and other avian influenza viruses has already given rise to multiple H9N2 viruses carrying new Hemagglutinin subtypes. Consequently, the aim of this study was to explore how many Hemagglutinin subtypes the H9N2 virus can carry and efficiently replicate with. To investigate this, the H9N2 avian influenza virus was engineered to encode different Hemagglutinin subtypes, in a procedure called reverse genetics. Here, each gene segment is physically mixed into a cocktail containing the complete virus genome. This cocktail is transferred into cells, which function as a factory to produce and replicate virus particles.

The H9N2 virus was able to produce infectious viral particles carrying ten out of ten Hemagglutinin subtypes tested. This highlights the flexibility of H9N2 for carrying different Hemagglutinin subtypes. Gladly, all variants of the H9N2 virus created replicated slower than the original H9N2 virus. This indicates that the H9N2 virus carrying a new Hemagglutinin subtype would not outcompete the original virus, if this virus appeared in nature. However, there are many factors that are not taken into account here, that could result in emergence of a H9N2 virus carrying a new Hemagglutinin subtype, despite it replicating slower.

KEY WORDS

Avian influenza virus, H9N2, HA subtypes, Reassortment, Reverse Genetics, Zoonosis

INTRODUCTION

Since 1900 there have been five global pandemics caused by influenza virus (1). Including the 1918 “Spanish Flu”, which was the single most fatal event in recorded history, causing an estimated 50 million human deaths worldwide (2). Influenza A virus (IAV) pandemics can cause infection in over 50% of an affected population in a single year and results in a major increase in excess mortality (1). Typically, after an IAV pandemic the strain continues to circulate at a lower level, causing annual seasonal outbreaks. Every year roughly 10% of unvaccinated adults are infected with seasonal IAV strains, causing an estimated 389 000 deaths globally (3, 4). As IAV vaccines need to be updated constantly to match the next seasons strain and the imminent pandemic threat posed by IAV, it remains a pathogen of major importance to global health and the economy (5).

The IAV genome consists of eight negative-sense single-stranded RNA gene (vRNA) segments, encoding ten viral proteins (6). The membrane proteins of IAV encompass Hemagglutinin (HA), Neuraminidase (NA) and M2. While the ribonucleoprotein complex of IAV consists of a vRNA segment coated in the proteins PB1, PB2, PA and NP. Additionally, multiple accessory proteins are expressed to enhance viral replication. Due to the segmented nature of the genome, vRNA segments from different IAVs can mix if a host is co-infected with two different IAVs. The process is named reassortment and can result in a genetic shift, where a novel IAV emerges. Most of the IAV pandemics in the past 120 years were attributable to genetic shift (1). The continued circulation of the pandemic strain as a seasonal IAV is due to genetic drift. Here, the high mutation rate of the viral polymerase combined with a selective pressure for immune escape mutants, rapidly selects for mutations in the surface antigens of the virus. These mutants effectively evade pre-existing immunity, facilitating re-infection of the host the following season and is the major reason why vaccines need to be continuously updated to match the seasonal strains (5, 7). The major surface antigens of IAVs are HA and NA (7).

The natural reservoir and origin of all IAVs infecting mammals are wild aquatic birds, mainly belonging to the order *Anseriformes* (swans, ducks, geese, etc.) and *Charadriiformes* (terns, gulls, etc.) (7). Avian influenza viruses (AIVs) mostly cause asymptomatic infections in wild aquatic birds and transmit through the faecal-oral route (7). In the AIV natural reservoir 16 HA (H1-H16) and 9 NA (N1-N9) subtypes have been characterised, accommodating a large antigenic diversity among AIVs, in wild aquatic birds (7). The prevalence of AIVs among wild birds is high, especially among ducks and geese, and reassortment is both common and necessary for AIV evolution (8–10). Only IAVs encompassing the H1, H2 and H3 subtypes have established stable lineages in humans, leaving the human population without immunity to the remaining 13 HA subtypes found in the natural wild bird reservoir (11). Consequently, reassortment between a seasonal human and wild bird AIV could result in the emergence of a zoonotic virus encoding novel surface antigens, which the human population is immunologically naïve to. The reassorted virus can then rapidly spread among the human population and potentially cause a pandemic (7). In fact, this is exactly how most IAV pandemics since 1900 have emerged (1).

AIVs from wild birds can readily infect mammals including humans, dogs, mink, horses, domestic pigs and sea mammals. However, these occasional spill over events from wild birds mostly cause sporadic infections and generation of stable IAV lineages are rare (7, 12). Since 1959, many sporadic cases and outbreaks of zoonotic AIVs have been reported globally, encompassing a variety of HA and NA subtypes (13). Interestingly, the source of most zoonotic

AIV infections are domestic birds belonging to the order *Galliformes* (e.g. chickens, quails, turkey, etc.) (7). Since the 1990's, circulation of multiple AIV subtypes in poultry have been reported, causing substantial economic losses to the poultry industry and international trade, whilst posing a public health risk (14). AIVs are grouped by their pathogenicity in chickens into low pathogenic AIV (LPAIV) and high pathogenic AIV (HPAIV). Most AIVs belong to the LPAIV group and are maintained in the aquatic wild bird reservoir. Further, no clinical symptoms manifest in infected wild birds and loss of body weight and reduced egg production is observed in infected domestic poultry. An example of a LPAIV that is currently circulating in poultry globally is the H9N2 AIV, which will be discussed in more detail below (15). To date, HPAIV only encompasses strains of the H5 and H7 subtypes and exhibits up to 100% mortality in various bird species (13). A dramatic example of a HPAIV outbreak is the HPAIV H5N1 first reported in 1997 in Hong Kong, transmitting from chickens to humans. The virus continued to spread globally and today it circulates in domestic poultry in Egypt and many countries in Asia (13). As of 2020, there have been 862 reported human cases of HPAIV H5N1 across 17 countries, with a case fatality rate of 53% (16). Interestingly, the HPAIV H5N1 derived its six internal gene segments (all gene segments except HA and NA) from co-circulating LPAIV H9N2 in poultry (17, 18).

The LPAIV H9N2 has been sporadically detected in poultry since the 1960's. However, an outbreak of H9N2 in domesticated chickens in China in the early 1990's continued to spread throughout the majority of Asia, the Middle East and North and West Africa, reaching panzootic proportions (8, 15). In part, the global spread of the LPAIV H9N2 in poultry has been overshadowed by the deadly HPAIV H5N1 outbreaks (8). Today, H9N2 has become the most prevalent LPAIV in poultry globally, co-circulating with HPAIV from H5 and H7 subtypes, giving rise to many opportunities for reassortment (15, 19). Poultry vaccination has been employed in various countries to curb the spread. However, due to genetic drift the vaccine seed strain has had to be updated in certain countries (15). Outbreaks of H9N2 in poultry can exhibit moderate to high morbidity and mortality, due to confounding factors like secondary bacterial and viral infections and poor nutrition and housing (15, 20). However, H9N2 is also frequently isolated from apparently healthy birds, suggesting that silent spreading plays a major role in poultry outbreaks (20). H9N2 readily infects humans, causing mild influenza-like symptoms. As of June 2019, there have been 59 laboratory-confirmed cases of H9N2 in humans (15). However, the trend has been increasing over the past few years. In majority of the confirmed cases, direct exposure to poultry was confirmed and there is no evidence of human-human transmission. More alarmingly however, sero-epidemiological studies in Asia report that human exposure to H9 might be a lot higher, especially among poultry workers (20, 21). In china, H9 sero-positivity rates in poultry workers was found to be up to 10% (22). Frequent human infections of H9N2 increases the chance of human adaptation and reassortment with human-adapted seasonal influenza virus strains (22). In fact, there is already evidence of human adaptation. Some H9N2 AIV isolates displays increased preference for "human-like" receptors and mutations in the PB2 gene, conferring enhanced replication in mammals (15, 23).

H9N2 presents a substantial zoonotic risk in its own right, however additional reassortment with seasonal human or avian influenza viruses could lead to emergence of strains with enhanced zoonotic and pandemic potential. As forementioned, the HPAIV H5N1 virus causing a deadly outbreak in Hong Kong in 1997 received its six internal gene segments from LPAIV H9N2 (17, 18). Interestingly, it seems that the H9N2 internal gene cassette (all gene segments except HA and NA) is highly compatible with various HA and NA subtypes, as this reassortment event has occurred multiple times in recent years. H9N2 has donated its complete

internal gene cassette to H1N2, H3N2, H5N2, H6N2 and H6N6 AIV (13). Further, reassortment has also given rise to human-infecting AIVs carrying the H9N2 internal gene cassette, including H5N6, H7N9 and H10N8 (24). Even though IAV reassortment is common in birds, reassorted viruses often display fitness defects and are outcompeted by the parental strains. This is due to segment mismatch, where heterologous viral components are incompatible after reassortment. IAV segment mismatch encompasses RNA mismatch and protein mismatch (25). To produce an infectious IAV particle, one copy of all eight vRNA segments must be packaged into one virion during IAV assembly. The current model suggests that vRNA segments form base-pairing interactions between adjacent vRNA segments, to selectively package one copy of each vRNA segment (25). This implies that distantly related IAV vRNA segments will assemble less efficiently, due to fewer RNA interactions between the heterologous vRNA segments, and this is the basis for RNA mismatch. However, even if the heterologous vRNA segments efficiently assemble into virions carrying all eight vRNA segments, the progenitor virus particle might exhibit fitness defects due to protein mismatches. This could be due to incompatibilities between the viral polymerase components PB2, PB1 and PA, leading to aberrant viral replication (25). Another example of protein mismatch is the functional balance that is required between HA and NA. During infection, HA binds the host cell surface receptor and facilitates cell entry. Upon virus exit NA complements the function of HA by destroying the surface receptors on the current host cell, to facilitate release of the newly formed virus particle. This means that the HA binding affinity and NA receptor cleavage activity must be functionally balanced, for optimal IAV infection (26). This would in part explain why the reassorted AIVs carrying the H9N2 internal gene cassette commonly receives HA and NA concurrently, from the donor virus (13).

AIM

In just under 30 years the H9N2 AIV has emerged, spread and established itself in poultry globally. Moreover, reassortment between H9N2 and other AIVs have already been detected in poultry and humans. Curiously, the internal gene cassette of H9N2 appears to be compatible with multiple HA and NA subtypes, in nature. Therefore, this study aimed to investigate the reassortment dynamics of HA subtypes in a poultry adapted H9N2 AIV. To investigate this, the study had four objectives:

1. Construct a panel of plasmids encoding a variety of HA subtypes
2. Investigate how many HA subtypes poultry adapted H9N2 AIV can reassort with
3. Assess the replicative fitness of the HA reassortants
4. Evaluate what impact the phylogenetic relationship between HA subtypes play on the replicative fitness of the HA reassortants

MATERIALS AND METHODS

Origin of virus isolates

The chicken H9N2 AIV, A/chicken/Egypt/S12568C/2016(H9N2), was kindly provided by Ahmed Mostafa from Giessen University, Germany. The complete genome was provided as eight separate plasmid constructs, where each gene segment was encoded on a pHW2000 plasmid. All wild bird AIV isolates used in the study for cloning HA gene segments were obtained from the Linnaeus University AIV repository (Jonas Waldeström) and isolated as described by Latorre-Margalef and colleagues (27). In short, viruses were isolated from mallards (or black-headed gull for the H16N3 isolate) captured at a long-term study site at Ottenby bird observatory, Sweden. Viruses were propagated in the allantoic cavity of 11-day old specific pathogen-free embryonated chicken eggs and harvested fluid was stored at −70 °C until further use.

NGS data assembly

The Next-Generation Sequencing (NGS) data for the wild bird AIV isolates used was kindly provided by Mahmoud Naguib from Uppsala University, Sweden. The data were re-analysed, to obtain the non-coding region in each HA gene segment. NGS data quality control was performed in FastQC (version 0.11.9) pre- and post-trimming. The NGS data was uploaded to Geneious Prime (version 2021.1.1) as Paired End Illumina data, with a read length of 150bp. Using the Trim Ends module, the overhangs from the forward (TCCCAGTCACGACGTCGT) and reverse (GGAAACAGC-TATGACCATG) primers were removed from the reads. Three mismatches, a minimal match length of eight nucleotides and "trim 5' and 3' end" was selected, with an error probability rate of 0.05. Next, a full-length HA nucleotide sequence from the same HA/NA subtype was collected from the NCBI influenza Virus Database, as reference sequence. The trimmed reads were mapped to the reference sequence using the Bowtie2 alignment method (Geneious Prime plugin: Bowtie), with local alignment and medium sensitivity selected. Lastly, the consensus HA sequence output was verified by nucleotide BLAST (NCBI). Due to the forward primer used during NGS library preparation encoding AGCG, all consensus sequence 5' ends were manually corrected to AGCA accordingly, post-assembly.

For the H16 subtype there was not NGS data available. Consequently, all full-length HA sequences originating from the same HA/NA subtype was collected from the NCBI influenza Virus Database. The resultant 245 nucleotide sequences were aligned directly in NCBI and the consensus 5' and 3' NCR was appended to the H16 CDS, to produce a full-length HA sequence.

Phylogenetics

The full-length nucleotide sequence of all HA subtypes was aligned in Geneious Prime. The Geneious Alignment method was utilised using global alignment with free end gaps, a cost matrix matching 51% similarity and a gap opening and extension penalty of 12 and 3, respectively. After alignment, a consensus tree was constructed from 1000 bootstrap trees, using the maximum likelihood method in IQ-Tree (28). All other settings were kept at default. An influenza B virus HA segment (GenBank accession: CY208184.1) was included in the analysis as an outgroup. The phylogenetic tree data was then uploaded to ITOL in Newick format, for annotating and displaying the tree (29).

Cloning HA subtypes into the pHW2000 plasmid

The pHW2000 plasmid was kindly provided by Martin Schwemmle from Freiburg University, Germany. The plasmid was transformed into competent DH5α cells (Invitrogen), using a standard heat shock protocol (30). The transformants were inoculated in 5ml LB containing 100µg/ml Ampicillin and incubated overnight at 37 °C. The culture was consequently miniprepped (Qiagen) and the purified plasmid was linearised using an Esp3I restriction enzyme (ThermoFisher). The linearised plasmid was run on a 1.2% agarose gel with a GelPilot 1kb plus DNA ladder (Qiagen), before being purified using a gel extraction kit (GeneJET). The pMKccdB plasmid was kindly provided by Ahmed Mostafa from Giessen University, Germany, and was amplified and linearised by Anishia Wasberg (31).

Primers for HA gene segment amplification were designed to encode ends compatible with the pHW2000 plasmid and nucleotides complementary to the specific HA subtype (figure. 1a). The H1 subtype isolate was not previously sequenced, so primers were designed according to a similar H1 sequence available from GenBank (Accession: JX565992.1). The strain had the same HA/NA subtype, host and isolation spot, but different isolation year. All primers were analysed for absence of strong secondary structures and appropriate GC content (40-60%) using an online primer analysis tool (OligoEvaluator, Sigma-Aldrich), before they were purchased (ThermoFisher) (figure. 1b).

Before cloning, Snapgene was used for *in silico* cloning of the HA segments. The "PCR" module in Snapgene was used to amplify the HA segment complementary DNA (cDNA) with the designed primers, restrict the HA cDNA and pHW2000 plasmid and ligate the HA cDNA into the pHW2000 plasmid (figure. 1c). This was subsequently used as a platform to align and analyse all sequencing results, post-cloning.

RNA extraction from the wild bird AIV isolates was performed using a QIAamp Viral RNA Kit (Qiagen), followed by RT-PCR to amplify the HA gene segment (SuperScript IV One-Step RT-PCR kit, ThermoFisher). A total of 10µl RNA extract was used as template, forward and reverse primers were as described above, and the annealing temperature was 58 °C. The HA cDNA was run on a 1.2% agarose gel, before purified using a gel extraction kit (GeneJET). The gel purified HA cDNA was restricted using BsmBI-v2 or BsaI-HFv2, according to the manufacturer's instructions (NEB). Then, PCR clean-up was performed on the restricted product (Nucleospin Gel and PCR cleanup columns, Macherey-Nagel). Further, 1µl of the restricted HA cDNA was run on another 1.2% agarose gel with a 1kb+ DNA ladder (see above), to confirm specific restriction. Next, the restricted HA cDNA was ligated into the linearised pHW2000 vector using a molar ratio of 1:3 of vector:insert and T4 DNA Ligase, according to manufacturer's instructions (NEB). However, the ligation was incubated for 16h at 16 °C. Next, 1-2µl of ligation mix was transformed into DH5α (ThermoFisher), XL-1 Blue (Agilent), Stbl3 (ThermoFisher) or HB101 (Promega) cells, following a standard heat shock protocol (30). After transformation, 100µl of cells were plated on an LB Agar plate containing 100µg/ml ampicillin (pHW2000) or 50µg/ml kanamycin (pMKccdB) and incubated at 37 °C overnight.

A colony PCR screening was performed to identify bacterial colonies encoding a full-length HA cDNA insert. In short, a colony was inoculated in 20µl nuclease-free H_2O and 9.2µl of the cell suspension was used as template for a 20µl PCR reaction (Platinum II Hot-Start PCR, Invitrogen). As a positive control, a sequence-verified DH5α pHW2000-H10 encoding isolate was inoculated. The PCR products were then run on a 1.2% agarose gel to separate full-length HA amplicons and HA amplicons containing large deletions. A GelPilot 1kb plus DNA ladder (Qiagen) was also included. Colonies encoding a full-length HA cDNA insert was inoculated (from the remaining cell suspension) in 3-5 ml LB and incubated overnight. The following day, 0.5ml of the culture was frozen at -80 °C, in a final concentration of 25% glycerol (v/v). The plasmid from the remaining culture was extracted using miniprep (Qiagen).

The purified plasmid was sent for sequencing (Mix2Seq, Eurofins), using a forward (GCTAACTAGAGAACCCACTGCTTAC) and reverse (GCGTTTTTGGGGACAGGTG) primer, complementary to the vector backbone (figure. 1c). The sequencing result was aligned to the *in silico* cloned pHW2000-HA construct, in Snapgene. After sequence verification, 200µl of the glycerol stock was inoculated in 250ml LB and incubated overnight. Next, the plasmids were extracted from the cultures using maxiprep (Plasmid Maxi Kit, QIAGEN) before another sequence confirmation. The sequence-verified, maxiprepped plasmid construct was used for transfection and virus rescue. All incubation steps were performed in LB containing 100µg/ml ampicillin (pHW2000) or 30µg/ml kanamycin (pMKccdB), at 37 °C with 180rpm shaking.

a)

b)

Primer name	Restriction enzyme	Nucleotide sequence (5' -> 3')
H1 forward	BsmBI-v2	GAGCCGTCTCAGGGAGCAAAAGCAGGGGAAAATCAAATCAATC
H1 reverse	BsmBI-v2	GAGCCGTCTCGTATTAGTAGAAACAAGGGTGTTTTTCC
H3 forward	BsmBI-v2	GAGCCGTCTCAGGGAGCAAAAGCAGGGGATACTTTCATTAATC
H3 reverse	BsmBI-v2	GAGCCGTCTCGTATTAGTAGAAACAAGGGTGTTTTTAACTATTAG
H4 forward	BsaI-HFv2	GATCGGTCTCGGGGAGCGAAAGCAGGGGAAACAATGCTATCAATTG
H4 reverse	BsaI-HFv2	GAGCGGTCTCGTATTAGTAGAAACAAGGGTGTTTTTTCTTCAAATG
H6 forward	BsmBI-v2	GATCCGTCTCGAGGGAGCAAAAGCAGGGGAAAATGA
H6 reverse	BsmBI-v2	GATCCGTCTCGTATTAGTAGAAACAAGGGTGTTTTTCTT
H8 forward	BsmBI-v2	GATCCGTCTCAGGGAGCAAAAGCAGGGGTCACAAT
H8 reverse	BsmBI-v2	GAGCCGTCTCGTATTAGTAGAAACAAGGGTGTTTTTTC
H10 forward	BsmBI-v2	GATCCGTCTCAGGGAGCAAAAGCAGGGGTCAC
H10 reverse	BsmBI-v2	GAGCCGTCTCGTATTAGTAGAAACAAGGGTGTTTTTAAC
H11 forward	BsmBI-v2	GAGCCGTCTCAGGGAGCAAAAGCAGGGGATTTATTAAGAAATC
H11 reverse	BsmBI-v2	GAGCCGTCTCGTATTAGTAGAAACAAGGGTGTTTTTGTCACAATTC
H12 forward	BsmBI-v2	GAGCCGTCTCAGGGAGCAAAAGCAGGGGTCACAATGG
H12 reverse	BsmBI-v2	GAGCCGTCTCGTATTAGTAGAAACAAGGGTGTTTTTAATTAAATAC
H15 forward	BsmBI-v2	GATCCGTCTCAGGGAGCAAAAGCAGGGGAAACAAAATGAAC
H15 reverse	BsmBI-v2	GAGCCGTCTCGTATTAGTAGAAACAAGGGTGTTTTTCAAATAATTATATACAG
H16 forward	BsaI-HFv2	GATCGGTCTCGGGGAGCAAAAGCAGGGGATATTGTCAAACAAAC
H16 reverse	BsaI-HFv2	GAGCGGTCTCGTATTAGTAGAAACAAGGGTATTTTTTCC

c)

Figure 1. Primer design, complete list of primers used for amplification of HA segments and an example of an *in silico* cloned pHW2000-HA plasmid construct. (**a**) The template for primer design, encoding four random terminal nucleotides for efficient restriction enzyme binding (yellow), followed by the recognition sequence for the BsmBI-v2 restriction enzyme (red). Alternatively, if a recognition site for BsmBI was already present within the HA segment, it was replaced by the recognition sequence for BsaI. Next, the primer encoded ends compatible with ligation into the pHW2000 vector, post-restriction (green), and 20-30 nucleotides of complementary sequence to the HA segment 5' or 3' end (black). Black arrows signify restriction site (4 nucleotide overhang is produced). (**b**) List of all primers designed as described in (a) and used to amplify the HA segments (column one). The accompanying restriction enzyme is displayed in column two and the sequence colour codes (column three) match the description in (a). (**c**) An example of an *in silico* cloned pHW2000-HA plasmid construct, encoding the H10 cDNA insert. The bidirectional promotors (grey arrows) and terminators (black boxes) flanking the H10 insert (green arrow), plus the primers used for sequencing the HA cDNA insert (pink arrows) is annotated. The plasmid was generated using Snapgene (Version 5.2.0) and the HA cDNA sequence was determined by NGS analysis (see "NGS data assembly").

Cell culture conditions and media

HEK293T and MDCK-2 cells (ATCC) were maintained in high-glucose DMEM (Gibco), supplemented with 1% (v/v) Antibiotic Antimycotic (Gibco) and 5% (v/v) foetal bovine serum (Gibco). All cell passaging and seeding of wells were kindly prepared by Anishia Wasberg. All media was preheated to 37 °C and cells were incubated at 37 °C with 5% CO_2, in a humidified incubator.

Co-transfection and virus rescue

A treated 6-well plate was seeded with co-cultured HEK293T and MDCK-2 cells at a 2:1 ratio, so that wells were 80-90% confluent on the day of transfection. The following day, all wells were washed 2x with DMEM and 1ml Opti-MEM (Gibco) was added to the well, before cells were incubated for 1 hour. In the meantime, the transfection reaction was prepared according to the manufacturer's instructions (Lipofectamine 3000 Transfection Reagent, ThermoFisher). However, 3.75µl Lipofectamine 3000 reagent and 500ng/plasmid was used for all transfections

and all mixtures were only carefully pipette mixed, without vortexing. The reaction included seven pHW2000 plasmids encoding the backbone of the chicken H9N2 AIV, mixed with one pHW2000 plasmid encoding an HA subtype. 6-12 hours post-transfection, the transfection media was replaced by 3ml infection media, per well. The infection media consisted of 0.2% (v/v) bovine albumin solution (MP Biomedicals), 1µl/ml TPCK treated Trypsin (Sigma-Aldrich) and 100u/ml Penicillin and 100µl/ml Streptomycin, diluted in Opti-MEM. 1ml virus-containing supernatant was collected from cells after 48 and 72h and immediately frozen at -20 °C. Before use, the virus-containing supernatant was thawed on ice and centrifuged at 1500x g for 10 min, to pellet cells. See "Cell culture conditions and media" for more info.

Virus propagation in embryonated chicken eggs

Specific pathogen-free embryonated chicken eggs were inoculated with virus, as described by Brauer and colleagues (32). In short, 200µl of centrifuged virus-containing supernatant was injected into the allantoic cavity of 10-day old embryonated chicken eggs (Håtunalab). Next, the infected eggs were incubated at 37 °C in an egg incubator, with >50% relative humidity. 3 days post-inoculation 5-13ml of allantoic fluid was harvested from the eggs and samples were streaked on a blood agar plate that was subsequently incubated overnight at 37 °C, to check for the presence of any bacterial contamination. The allantoic fluid was frozen at -20 °C for short-term storage. After confirmation of virus in the sample by a hemagglutination assay and RT-qPCR, the allantoic fluid was thawed on ice and centrifuged at 1000x g for 10 min at 4 °C. The centrifuged allantoic fluid was consequently aliquoted and frozen to -80 °C, until further use.

Hemagglutination assay

The hemagglutination assay was performed according to the guidelines set by the OIE Terrestrial Manual (33). In short, 25µl of virus-containing allantoic fluid was serially diluted 2-fold across a V-shaped 96-well plate containing 25µl 1x PBS, leaving the last column without virus as a control. This was done in duplicates for each virus. Next, 25µl of 1% (v/v) fresh chicken blood (Håtunalab) in 1x PBS was added to all wells. After 20 min of incubation at room temperature, the plate was tilted 45° to allow the pelleted red blood cells (RBC) to stream into a teardrop shape. Any well not exhibiting an RBC pellet or a streaming teardrop of the RBC pellet was recorded as positive for virus. The HA titre (the highest dilution factor positive for virus) was then recorded for each virus.

RT-qPCR

RNA extraction from virus-containing allantoic fluid was carried out using a Maxwell 16 RNA extraction instrument, according to manufacturer's instructions (AS1000, Promega). Next, the HA segment of each reassortant virus was verified by RT-qPCR, using the CFX Connect thermocycler and CFX Manager software (Bio-Rad). An AgPath-ID One-Step RT-PCR kit was utilized, according to the manufacturer's instructions (Applied Biosystems). The primers and fluorescent probes used originated from an influenza HA subtype panel, developed by Timm Harder from Friedrich-Loeffler-institut, Germany. The panel was designed to amplify a particular HA subtype specifically (unpublished). The thermocycler settings were according to the manufacturer's instructions, but an annealing temperature of 56 °C, 40 cycles and a FAM fluorophore was used on all channels analysed. Fluorescent drift correction was enabled in the CFX Manager and the original AIV isolate RNA that the particular HA subtype was cloned from was included as a positive control.

Virus titration

MDCK-2 cells were seeded in a treated 96-well plate, so that wells were 80-90% confluent on the day of infection (cell plate). The following day, 20µl of virus-containing allantoic fluid was

serially diluted 10-fold across a 96-well plate, containing 180µl of DMEM (virus dilution plate). The cell plate was washed 1x in DMEM, before 100µl from the virus dilution plate was added to the corresponding well on the cell plate. The cells were incubated for 1h, before the inoculum was replaced by 100µl of infection media diluted in DMEM, as described above. Cells were incubated for 72h, before a hemagglutination assay was performed, as described in "Hemagglutination assay". However, 25µl of virus-containing supernatant from the cell plate was added to the corresponding well in the V-shaped 96-well plate containing 25µl 1x PBS, without further dilutions. Each virus was titrated in triplicates and the 50% Tissue Culture Infectious Dose per ml ($TCID_{50}$/ml) was calculated from the proportion of hemagglutination positive wells per dilution, using the Spearman and Kärber algorithm (described in 37). Data was plotted for each time point, using the ggplot2 package in Rstudio (35; Rstudio version 1.0.143). See "Cell culture conditions and media" for more info.

Replication kinetics

MDCK-2 cells were seeded in a treated 24-well plate, so that the cells were 80-90% confluent on the day of infection. In parallel, all viruses were diluted to 1000 $TCID_{50}$/ml in DMEM. To verify equal concentrations of virus, RNA extraction of diluted viruses was performed, using the Maxwell 16 RNA extraction instrument (AS1000, Promega). Next, RT-qPCR was performed with primers and a probe targeting the M gene segment, as described above (AgPath-ID™ One-Step RT-PCR, Applied Biosystems). Samples with C_q values outside the standard deviation from the mean of all samples was corrected for accordingly (Table 1). The following day, all wells of the 24-well plate were washed 1x with DMEM. Then cells were inoculated with 200µl of the diluted virus (Table 1, column 3) and incubated for 1h, before virus inoculum was replaced by 200µl of infection media in DMEM, as described above. Cells were incubated for 72h, while supernatant was collected at 4, 24, 48 and 72 hours post-inoculation and frozen at -20 °C. The experiment was performed in triplicates and media and cell incubation conditions were as described above. RNA extraction of supernatants was carried out using the QIAamp mini viral RNA kit (Qiagen), before a RT-qPCR with primers and a probe targeting the M gene was performed, as described above (AgPath-ID™ One-Step RT-PCR, Applied Biosystems). The primers and probes were also designed by Timm Harder from Friedrich-Loeffler-institut, Germany. Lastly, the C_q values for all samples were normalised to 0 for the 4h timepoint. Next, the negative change in C_q value over time ($-\Delta C_q$) was plotted. Normal distribution and equal variance within data was checked, before a One-Way ANOVA was performed to test for significant differences between viruses 72 hours post-inoculation. All statistics and the graph were made using Rstudio and the ggplot2 package. See "Cell culture conditions and media" for more info.

Table 1. Normalisation of a selected subset of the chicken H9N2(HA) reassortants, according to viral titre. Selected reassortants (column 1) were diluted to 1000 $TCID_{50}$/ml and a RT-qPCR was performed to verify equal copy numbers between the reassortants (column two). Any reassortant with a C_q value outside the mean±SD was adjusted for (column three).

Virus	C_q value for 1000 $TCID_{50}$/ml	Final dilution ($TCID_{50}$/ml)
H9N2	27.34	10000
H9N2(H6)	15.92	1000
H9N2(H10)	18.65	1000
H9N2(H11)	17.68	1000
H9N2(H12)	14.46	500
H9N2(H15)	16.45	1000
Mean ± SD	**18.42±4.60**	

RESULTS

Obtaining the full-length nucleotide sequence of the HA subtypes

All the HA subtypes included in the study, except H1, were already sequenced and deposited in GenBank. However, most of them lacked their Non-Coding Region (NCR) or only included a partial Coding Sequence (CDS). To obtain the full-length sequence of all HA subtypes included in the study, the NGS data from their respective wild bird AIV isolates was reassembled in Geneious Prime. The purpose was to have the most accurate data to perform phylogenetic analysis with and to ensure accurate primer design for amplification of the HA segments, during cloning. In short, quality control was performed on the Illumina NGS data, before the reads were trimmed and assembled to reference sequence in Geneious Prime. A full-length HA sequence originating from an isolate with a matching HA/NA subtype was used as reference sequence. The resulting consensus sequence was verified by nucleotide BLAST.

The full-length nucleotide sequence of the HA subtypes H3, H4, H6, H8, H9, H10, H11 and H15 were successfully obtained by NGS assembly in Geneious Prime. All consensus sequences displayed correct CDS compared with the published sequence and consistent NCR with other highly related HA sequences, when evaluated by nucleotide BLAST (data not shown). For the H8 consensus sequence, one nucleotide was found to be incorrect in the published sequence and was corrected for accordingly (G390T). This was verified by Sanger sequencing of the H8 cDNA insert, post-cloning (data not shown). To obtain the nucleotide sequence for the H1 subtype (that was not previously sequenced), the HA cDNA insert was Sanger sequenced post-cloning. For the H16 subtype there was no NGS data available. To circumvent this, the consensus NCR of H16 sequences from the NCBI influenza virus database was appended to the H16 CDS, to produce a full-length HA sequence. This was verified by Sanger sequencing of the H16 cDNA insert, post-cloning. The full-length nucleotide sequence of H12 was already available in GenBank.

In summary, the full-length nucleotide sequence for the HA subtypes H1, H3, H4, H6, H8, H9, H10, H11, H15 and H16 was obtained, through NGS analysis, Sanger sequencing or consensus sequence from an alignment of similar sequences.

HA subtypes with similar genotypes cluster into distinct HA clades and groups

To determine the phylogenetic relatedness between all HA subtypes included in the study, a phylogenetic tree of the HA subtypes was constructed.

The tree consisted of two groups, which could be further subdivided into five clades (fig. 2). Group 1 consisted of the H3 clade (lime colour, H3 and H4) and the H10 clade (green colour, H10 and H15). Group 2 consisted of the H1 clade (pink colour, H1 and H6), the H11 clade (blue colour, H11 and H16) and the H9 clade (red colour, H8, mallard H9, chicken H9 and H12). All clades were well supported (>90% bootstrap support), but group 2 had a 64% bootstrap support. The unique colour assigned to each HA subtype was used throughout the report, to signify the HA clade the subtype belongs to.

Overall, the HA subtypes clustered into distinct HA clades and groups, based on their phylogenetic relatedness.

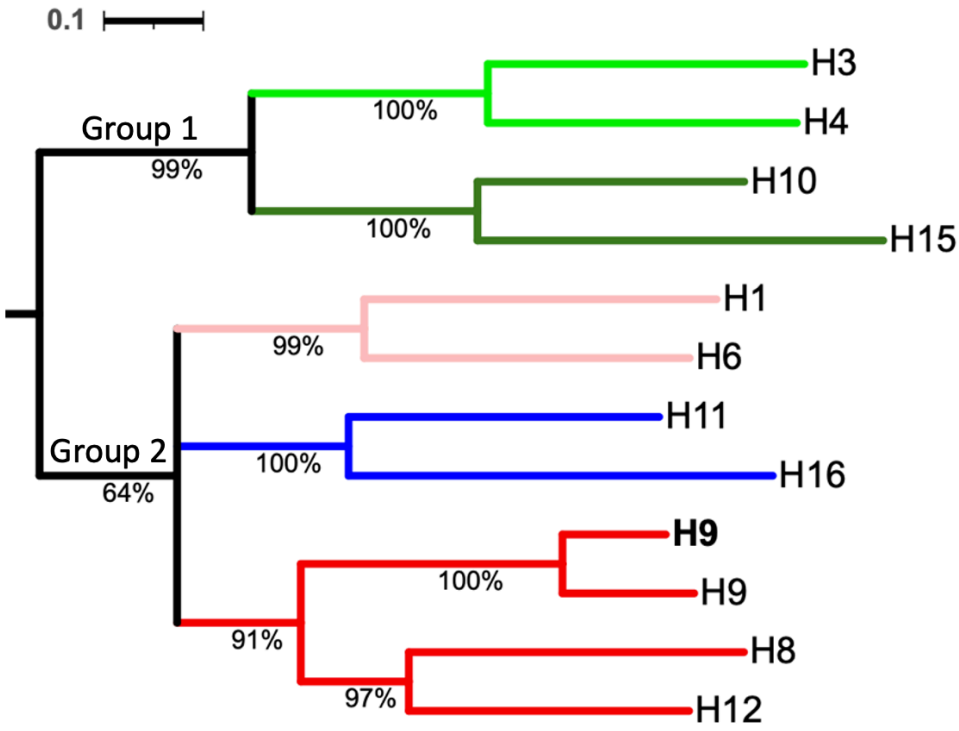

Figure 2. Phylogenetic relatedness between all HA subtypes included in the study. The cDNA sequence from all HA subtypes included in the study was aligned in Geneious Prime. Then, a consensus tree was constructed from a 1000 bootstrap trees, using the Maximum Likelihood method in IQ-Tree. The final tree was annotated and displayed using ITOL, where each HA clade was assigned a unique colour. Scalebar signifies substitutions per site, % value signifies bootstrap support of each clade, and an influenza B virus HA segment was included to root the tree (not shown). All HA subtypes originate from mallards, except for H16 that was isolated from black-headed gulls and H9 (bold) that was isolated from chickens.

Ten out of eleven available HA subtypes were successfully cloned

The first objective of the study was to construct a panel of plasmids, encoding a variety of HA subtypes. These would later be used to rescue the chicken H9N2 AIV, using a plasmid-based reverse genetics system. Therefore, HA segments from wild bird AIV isolates, encompassing most HA subtypes, were cloned into a pHW2000 bidirectional expression plasmid. In short, HA gene segment cDNA was amplified from AIV isolates using RT-PCR, and the pHW2000-HA construct was transformed into DH5α cells. Single colonies were screened for a full-length HA gene insert by colony PCR and positive colonies were subsequently sequenced.

Initially, no bacterial transformants were obtained after transformation of the plasmid construct. After troubleshooting, it was established that changing to the T4 DNA ligase kit supplied by NEB, in combination with overnight incubation of the ligation reaction, resulted in high yields of transformants (data not shown). However, seven out of the ten HA subtypes cloned encoded unstable cDNA sequences that led to large deletions (~1kb) in the HA cDNA insert, after transformation into competent DH5α cells (Fig. 3a). This was not detected for the H4, H6 and H11 subtypes, suggesting their cDNA sequence was stable in DH5α cells. However, the remaining HA subtypes displayed large deletions in the HA cDNA insert, in at least 33% of the screened colonies. This was particularly apparent for the H8 subtype, where 70 screened colonies all exhibited large deletions in the H8 cDNA insert.

To obtain a clone encoding the full-length H8 gene segment, the pHW2000-H8 construct was transformed into XL-1 Blue, Stbl3 and HB101 competent cells, incubated at 37 °C and 10, 20 and 19 colonies were screened by colony PCR, respectively. All screened colonies exhibited large deletions in the H8 cDNA insert (data not shown). However, the pHW2000-H8 (28 colonies screened) and the pMKccdB-H8 (30 colonies screened) construct

transformed into HB101 competent cells and incubated at 30 °C both yielded one colony each, encoding the full-length H8 cDNA insert (data not shown). Unfortunately, sequencing revealed that both constructs incorporated a single nucleotide insertion or deletion, leading to a frameshift mutation in the H8 CDS (Fig. 3b). Curiously, both mutations were located within 26 bases of each other. Consequently, cloning of the H8 subtype was not pursued further.

After selection of colonies encoding a full-length HA segment in the pHW2000 plasmid, there were generally no mutations after sequencing, excluding the problematic H8 subtype (data not shown). Ten out of eleven available HA subtypes from wild bird AIV isolates were successfully cloned into the pHW2000 bidirectional expression plasmid (Fig. 3c).

a)

HA subtype cloned into pHW2000 and transformed into DH5α	Proportion of screened colonies exhibiting large deletions (~1kb) in the HA insert
H1	2/6 (33%)
H3	3/6 (50%)
H4	0/6 (0%)
H6	0/5 (0%)
H8	70/70 (100%)
H10	6/10 (60%)
H11	0/3 (0%)
H12	3/6 (50%)
H15	1/3 (33%)
H16	2/6 (33%)

b)

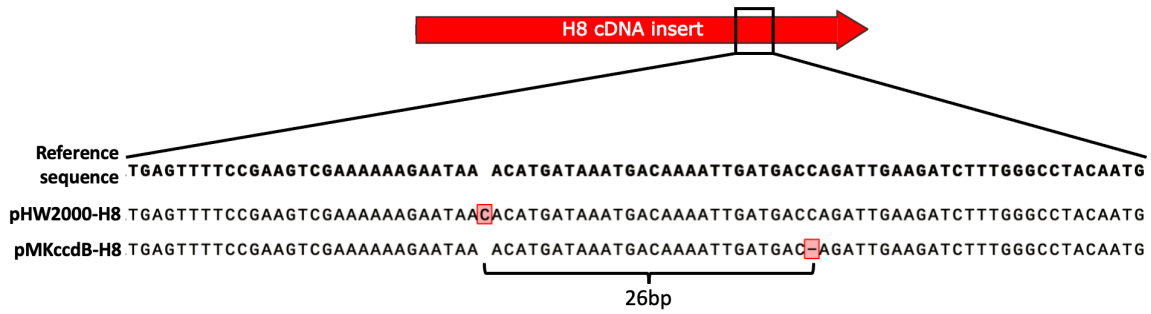

c)

HA subtypes cloned	Original strain of HA segment
H1	A/Mallard/Sweden/51833/2006(H1N1)
H3	A/Mallard/Sweden/101487/2009(H3N8)
H4	A/Mallard/Sweden/80148/2008(H4N6)
H6	A/Mallard/Sweden/99825/2009(H6N2)
H9*	A/Mallard/Sweden/67860/2007(H9N2)
H10	A/Mallard/Sweden/102087/2009(H10N1)
H11	A/Mallard/Sweden/102103/2009(H11N9)
H12	A/Mallard/Sweden/100127/2009(H12N5)
H15	A/Mallard duck/Sweden/139703/2012(H15N5)
H16	A/Black-headed gull/Sweden/74340/2008(H16N3)

Figure 3. Proportion of screened colonies exhibiting large deletions in the HA cDNA insert post-transformation, sequencing result for the full-length H8 cDNA constructs obtained and overview of all cloned HA subtypes. (**a**) The HA gene segment from different AIV subtypes was amplified and cloned into a pHW2000 plasmid. Next, the plasmid was transformed into DH5α competent cells, for selection and amplification (first column). However, some HA subtypes encoded unstable cDNA that resulted in large deletions (~1kb) in the HA cDNA insert. Individual colonies of DH5α cells transformed with pHW2000-HA constructs were screened for a full-length HA cDNA insert by colony PCR or sequencing. The proportion of colonies exhibiting large deletions in the HA cDNA insert was then recorded (second column). (**b**) Sequencing results for the full-length pHW2000-H8 and pMKccdB-H8 constructs obtained by transformation in HB101 competent cells at 30 °C, aligned against the H8 cDNA reference sequence in Snapgene. Illustrates that the nucleotide insertion (pHW2000-H8) and deletion (pMKccdB-H8) in the two independent colonies are in close proximity. (**c**) Overview of all successfully cloned HA subtypes into the pHW2000 plasmid (first column) and the AIV isolate origin for the HA segment (second column). * The H9 mallard subtype was cloned by Anishia Wasberg, using the same method.

The chicken H9N2 AIV was compatible with ten out of ten HA subtypes cloned

The second objective of the study was to investigate how many HA subtypes chicken H9N2 AIV can reassort with (Fig. 4a, step I). This was achieved by employing an eight-plasmid reverse genetics system, where each influenza gene segment was encoded on a separate pHW2000 plasmid (36). In the cell, all gene segments are simultaneously transcribed into vRNA and mRNA and the cell assembles and propagates infectious IAV particles. Seven plasmids encoding the chicken H9N2 AIV backbone was co-transfected with one plasmid encoding an HA subtype, originating from wild bird AIV isolates (Fig. 4a, step II-III). Further, each rescued virus was propagated in embryonated chicken eggs, to increase viral titres (Fig. 4a, step IV). Each reassortant virus is annotated as H9N2(HA), where (HA) signifies the HA subtype encoded by the virus.

Allantoic fluid from all chicken H9N2(HA) reassortants displayed hemagglutination activity after the first rescue attempt, except for the H9N2(H9) and H9N2(H16) reassortant (Fig. 4b). Rescue of the chicken H9N2(H9) was repeated two times and no hemagglutination activity was observed. Rescue of the chicken H9N2(H16) reassortant was repeated three times and hemagglutination activity was observed 72 hours post-transfection, in one repeat. When the HA titre was recorded 48 and 72 hours post-transfection, the sample with the highest HA titre was used for all downstream experiments.

Next, RT-qPCR amplification of the respective HA subtype in all chicken H9N2(HA) reassortants was successful, including the chicken H9N2(H9) reassortant that was negative for hemagglutination activity (Fig. 4c). The C_q values ranged from 10 to 14 for all viruses, except for the H9N2(H9) reassortant that had a C_q value of 27.31. Due to low yields of the chicken

H9N2(H9) reassortant, it was not included in subsequent experiments. All chicken H9N2(HA) reassortants tested negative for other HA subtypes (data not shown).

Unsurprisingly, the wild-type chicken H9N2 virus yielded the highest viral titre, after rescue (Fig. 4d). However, the H9N2(H12) reassortant yielded one of the lowest viral titres, despite its HA subtype belonging to the same HA clade as H9. Moreover, there were large differences in viral titres between reassortants within the same HA clade (Fig. 4d, see the lime, blue and red HA clades).

In summary, the chicken H9N2 AIV was compatible with all the cloned HA subtypes of this study, producing infectious viral particles after transfection. Nonetheless, the chicken H9N2(H16) reassortant only produced detectable virus 72 hours post-transfection. Moreover, the chicken H9N2(H9) reassortant was only detected by RT-qPCR, exhibiting few viral copies. Lastly, rescue of the wild-type H9N2 virus was most efficient, and the viral titres achieved after rescue were not correlated with the HA clades the HA reassortants belonged too.

a)

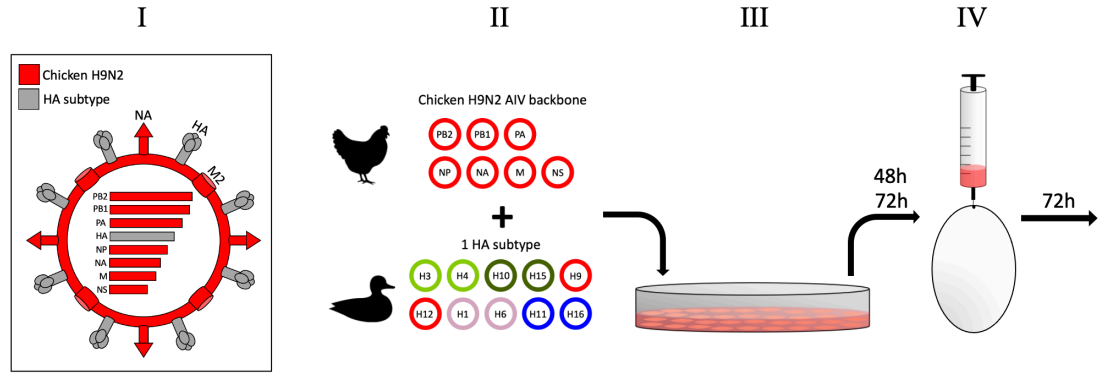

b)

Virus	HA titre 48h	HA titre 72h
H9N2	128	
H9N2(H1)	16	32
H9N2(H3)	128	
H9N2(H4)	32	128
H9N2(H6)	1024	128
H9N2(H9)	0	0
H9N2(H10)	128	
H9N2(H11)	64	32
H9N2(H12)	128	
H9N2(H15)	1024	
H9N2(H16)	0	32

c)

Virus	RT-qPCR target	C_q value
H9N2	H9	10.01
H9N2(H1)	H1	13.96
H9N2(H3)	H3	11.21
H9N2(H4)	H4	12.51
H9N2(H6)	H6	12.87
H9N2(H9)	H9	27.31
H9N2(H10)	H10	12.65
H9N2(H11)	H11	10.95
H9N2(H12)	H12	11.10
H9N2(H15)	H15	11.17
H9N2(H16)	H16	13.49

d)

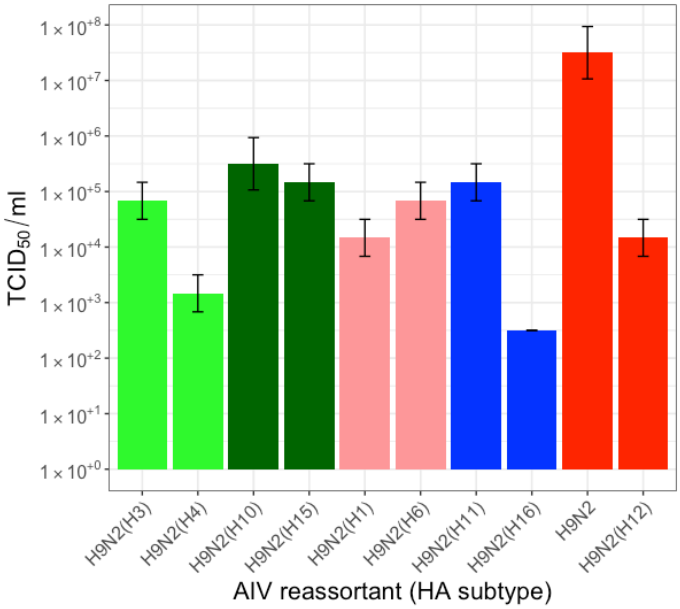

Figure 4. Aim and workflow for rescue of the chicken H9N2(HA) reassortants, confirmation of successful rescue and virus titration of rescued HA reassortants. (**a**) The aim was to rescue the chicken H9N2 AIV with different HA subtypes (step I). To achieve this, seven plasmids encoding the chicken H9N2 AIV backbone (all gene segments excluding HA) were mixed with one plasmid encoding an HA subtype, from wild bird AIV isolates (step II). The plasmids were co-transfected in co-cultured HEK293T and MDCK-2 cells and the virus-containing supernatant was collected 48 and 72 hours post-transfection (step III). Next, the virus-containing supernatant was injected into the allantoic cavity of 10-day old specific pathogen-free embryonated chicken eggs and the allantoic fluid was harvested 72 hours post-inoculation (step IV). (**b**) Presence of virus after co-transfection and propagation in embryonated chicken eggs was confirmed by a hemagglutination assay. The HA titre (highest dilution factor giving positive hemagglutination) was recorded 48 and/or 72 hours post-transfection, for each chicken H9N2(HA) reassortant. Each virus was tested in duplicates, in 1% fresh chicken blood. (**c**) RT-qPCR with primers and a FAM fluorescent probe targeting specific HA subtypes was utilised (column two) on RNA extracts from all chicken H9N2(HA) reassortants (column one). Cycle quantification (C_q) value signifies the number of cycles required to pass the C_q threshold (column three). As a positive control, the AIV isolate the HA subtype was cloned from was also amplified with the same RT-qPCR master mix and as a negative control the RNA template was replaced with nuclease-free H_2O (data not shown). (**d**) Virus titration of the rescued chicken H9N2(HA) reassortant viruses. 10-fold dilutions of each reassortant virus were inoculated on a monolayer of MDCK-2 cells for 1h, before the inoculum was replaced with infection media. 72 hours post-inoculation, a hemagglutination assay was performed on the supernatant from each infected well and the $TCID_{50}$/ml was calculated using the Spearman and Kärber algorithm. Each virus was titrated in triplicates and the error bars signify the standard deviation, calculated by the same method. The plasmids in (a) and bars in (d) are coloured according to the HA clade the HA subtype belongs too (see Fig. 2). Each chicken H9N2 reassortant virus is annotated as H9N2(HA), where HA signifies the HA subtype encoded by the virus.

The HA reassortants displayed lowered replicative fitness, independently of their HA clade

The third and fourth objective of the study was to assess the replicative fitness of the HA reassortants and evaluate what impact the phylogenetic relationship between HA subtypes play on the replicative fitness of the HA reassortants. To investigate this, the replication kinetics of a selected subset of the HA reassortants, covering most HA clades, was assessed. Firstly, the HA reassortants were normalised by viral titre, so that the infectious dose would be equal (Table 1). Then MDCK-2 cells were infected with the HA reassortants and supernatant was collected at different timepoints, followed by RT-qPCR to quantify viral RNA copies.

The wild-type chicken H9N2 virus displayed a significantly larger decrease in C_q value over time, compared to the HA reassortants (Fig. 5). This suggests that the wild-type virus

displayed the highest replicative fitness in MDCK-2 cells. Interestingly, the fittest reassortant virus was the chicken H9N2(H10), which HA subtype belongs to another HA clade and group (Fig. 5; Fig. 2). Moreover, the chicken H9N2(H12) reassortant displayed significantly lower replicative fitness than all tested HA reassortants, despite belonging to the same HA clade as the original H9. Lastly, there was no significant difference between the replicative fitness of the chicken H9N2(H11), H9N2(H15) and H9N2(H6) reassortants, all belonging to separate HA clades. The mock infection for all viruses did not display any amplification (data not shown).

In conclusion, the wild-type chicken H9N2 AIV displayed the highest viral replicative fitness in MDCK-2 cells. Additionally, there was no correlation between the phylogenetic relationship of the HA subtypes and the replicative fitness of the HA reassortants.

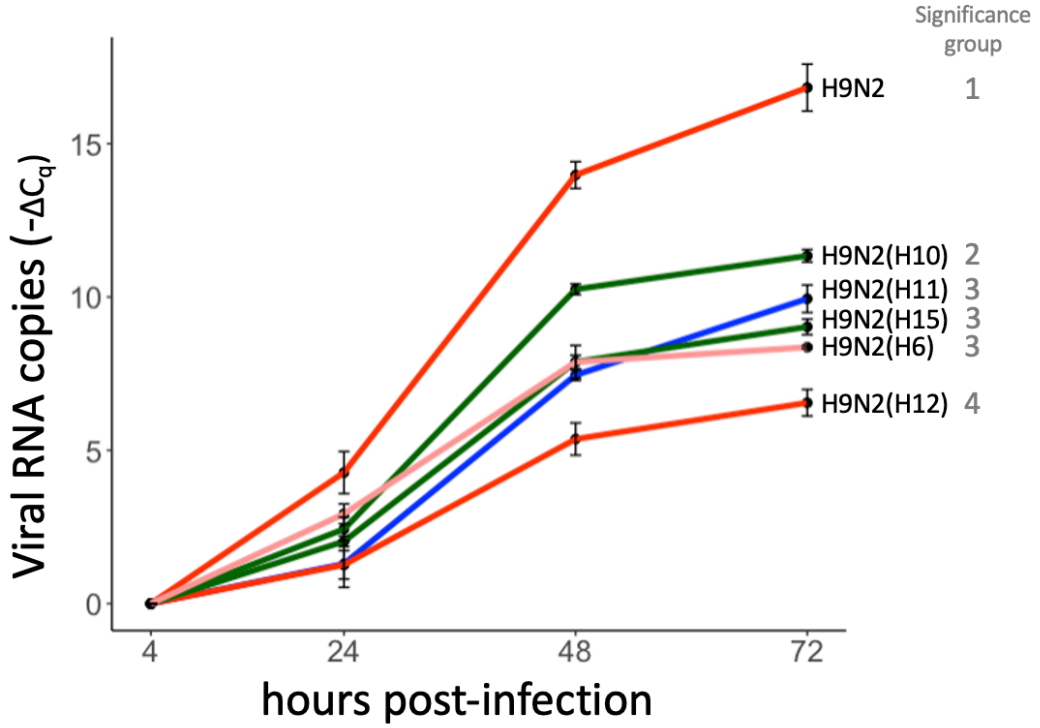

Figure 5. Replication kinetics for a subset of the chicken H9N2(HA) reassortants. The diluted viruses were inoculated on a monolayer of MDCK-2 cells for 1h, before the inoculum was replaced with infection media. Virus-containing supernatant was collected at different timepoints, followed by RNA extraction. Finally, RT-qPCR with primers and probes targeting the M gene segment was carried out, to quantify the change in viral RNA copies over time. Each virus was inoculated in triplicates, plus a mock infection for each virus which was collected after 72h (data not shown). Error bars signify standard deviation from mean and y-axis shows negative change in C_q value after the first time point ($-\Delta C_q$), where a higher number signifies a higher increase in viral RNA copies. Statistical significance was calculated by a One-Way ANOVA test, after assumptions were tested. Reassortants with different grey numbers next to them are significantly different from each other at 72h ($p<0.001$). Statistics was carried out using Rstudio. All lines are coloured according to the HA clade the HA subtype belongs too (see Fig. 2).

DISCUSSION

The majority of HA subtypes encode toxic cDNA that promotes recombination in *E. coli*

With over 1500 citations in Google Scholar (accessed 07.05.2021), the reverse genetics system based on the pHW2000 bidirectional expression plasmid is a popular choice for quick and efficient generation of recombinant influenza viruses (36). Remarkably, there is scarce literature concerning the genetic instability of some IAV gene segments when cloned and transformed into *E. coli* (three studies were found, discussed below). Here, I report for the first time that genetic instability is common across many HA subtypes. My data demonstrates that seven out of the ten HA subtypes cloned frequently displays large deletions in the HA cDNA insert, after transformation into competent *E. coli* (Fig. 3a). In addition, the H9 mallard subtype cloned by Anishia Wasberg also exhibited large deletions (personal communication). Even when employing various recombinase deficient *E. coli* strains, large deletions in the HA cDNA insert were still observed. This genetic instability suggests that some HA subtypes encode a cDNA sequence that is toxic to the bacteria, as that there is a strong selective pressure to delete large regions of the sequence.

A literature search revealed three studies addressing the issue of genetic instability of IAV gene segments and how to overcome this during cloning (37–39). They report that using a low-copy plasmid alternative, using the HB101 competent *E. coli* strain or lowering the incubation temperature, reduces the frequency of recombination and stabilises the cloned sequence. Consequently, the highly unstable H8 cDNA was cloned into a low-copy plasmid, pMKccdB, the construct was transformed into HB101 competent cells and the bacteria was incubated at 30 °C. These modifications enabled isolation of two colonies without large deletions in the H8 cDNA insert, supporting the notion that one or a combination of these methods reduces the frequency of recombination.

However, both colonies incorporated frameshift mutations in the H8 CDS (Fig. 3b). One report addressing the issue proposes that the toxicity of the IAV gene segments in *E. coli* is due to expression of toxic gene products, presence of AT-rich sequences, a high plasmid copy number, secondary DNA sequence structures or presence of long repeats or promotors (37). It has also been reported that the Cytomegalovirus promoter, driving transcription of the inserted IAV gene segment (see CMV promoter in Fig. 1c), has transcriptional activity in *E. coli* (40). Since the two frameshift mutations were found in close proximity near the 3' end of the H8 CDS, I suggest that the genetic instability is due to expression of the HA protein in *E. coli*, which is toxic to the cells (Fig. 3b). This is also consistent with the other report, where the few colonies they isolated encoding the full-length H9 subtype cDNA, contained frameshift mutations (37). To test this hypothesis, one could incorporate a frameshift mutation early in the H8 CDS, before transformation. If this construct displays a reduced frequency of large deletions compared to the native H8 CDS, it would strongly suggest that the HA protein is expressed and toxic in *E. coli*. If this is the case, one could modify the pHW2000 plasmid so that the CMV promoter is under control of an inducible repressor, to ensure that the HA gene is silenced during amplification in *E. coli*.

Ultimately, ten out of sixteen HA subtypes from AIV in wild birds was successfully cloned into the pHW2000 bidirectional expression plasmid (Fig. 3c). The remaining HA subtypes, except H8, was not cloned due to biosafety reasons (H5 and H7 displaying a highly pathogenic phenotype) or that an IAV isolate encoding the HA subtype was not available (H2, H13 and H14).

The chicken H9N2 AIV is highly compatible with different HA subtypes

Genetic diversity between HA subtypes is high, while genetic diversity within an HA subtype is relatively low (9). This pattern can be explained by the allopatric and sympatric models of speciation (9). The allopatric model propose that HA segments became geographically- and host-isolated and diverged into discrete HA subtypes, over time. In this scenario, HA subtypes would also functionally diverge over time and eventually not be compatible anymore. While the sympatric model propose that HA segments evolved within the same spatial population and natural selection favoured divergence of the HA segments into discrete HA subtypes. In this scenario, natural selection would favour mutations in the antigenic site first, to reduce cross-immunity between different HA segments. At the same time, there would be a selective pressure to retain the functional compatibility of the different HA segments, to ensure that reassortment produces viable viral progeny. This would result in a pool of discrete but compatible HA subtypes within the viral population, facilitating reassortment and evasion of pre-existing immunity in the wild bird host (9). Here, I demonstrate that rescue of the chicken H9N2 AIV is highly efficient with eight out of ten HA subtypes cloned, as infectious viral particles were detected after just one co-transfection attempt (Fig. 4b and c). This supports the sympatric model of speciation, as majority of the cloned HA subtypes are functionally compatible with the chicken H9N2 AIV backbone, despite divergent sequences.

However, the H9 and H16 subtype cloned were inefficient at rescuing the chicken H9N2 AIV. This raises the question whether this was due to low segment compatibility with the chicken H9N2 AIV or if these HA subtypes are generally incompatible with AIV reassortment. For the H9 subtype, the allopatric model of speciation is highly implausible since it belongs to the same HA subtype as the chicken H9 segment. However, there is evidence to suggest that it is generally less compatible with reassortment. A large-scale phylogenetic study of the reassortment patterns within the Eurasian AIV pool found that the H9 subtype had a lower reassortment rate than the H1-H4 subtypes (41). For the H16 subtype, it is noteworthy that this is the only HA subtype cloned not originating from mallard, but from black-headed gulls (Fig. 3c). In fact, most AIV isolates encoding the H16 subtype are isolated from gulls (42). This would suggest that the H16 subtype has been isolated from the highly diverse AIV pool, found predominantly in wild ducks (42). Therefore, the inefficiency of the H16 subtype to rescue the chicken H9N2 AIV could be explained by the allopatric model of speciation, where host-isolation has led to functional divergence of the H16 subtype over time.

Another study, aimed to rescue the A/PR/8/34(H1N1) IAV backbone with all 16 HA subtypes, employed an almost identical approach to the one described here, allowing for some interesting comparisons (43). Firstly, they were also unable to rescue the H9 and H16 subtypes in the H1N1 backbone, through co-transfection in HEK293T cells followed by serial passages in MDCK cells supplemented with Trypsin. They found that additionally treating the cells with neuraminidase and over-expressing the polymerase complex with additional helper plasmids was required to rescue the H1N1 backbone with H9. However, this approach did not enable rescue of the H1N1 backbone with the H16 subtype (which coincidentally was also isolated from black-headed gulls from Sweden). In this instance, they found that directly injecting resuspended HEK293T cells into embryonated chicken eggs, after co-transfection, resulted in successful rescue and virus production. They also state that H16 subtype viruses generally grow poorly in MDCK cells. Altogether, this suggests that it is generally difficult to rescue IAV backbones with the H9 or H16 subtype from wild bird AIV isolates.

Ultimately, the chicken H9N2 AIV produced infectious viral particles encoding all ten HA subtypes (Fig. 4c). In combination with the current literature, this suggests that the H9N2 AIV backbone is compatible with at least twelve out of sixteen HA subtypes, from wild bird AIVs (18, 43, Fig. 4c). Nonetheless, all HA reassortants yielded viral titres >100-fold lower than the wild-type virus, suggesting that rescue of heterologous HA subtypes is generally less

efficient (Fig. 4d). Especially the H9 subtype from mallard, as very few viral copies were detected (Fig. 4c). The reason for this remains unelucidated here and should be investigated further.

In conclusion, my data supports the sympatric model of speciation of HA subtypes and the hypothesis by Dugan et al., that wild bird AIVs exist as a large pool of functionally equivalent gene segments that are interchangeable (9). Nevertheless, the H16 subtype highlights that the allopatric model of speciation also plays some role in AIV evolution and diversity, as suggested by Dugan et al. (9).

The HA reassortants displayed lowered replicative fitness due to segment mismatch and HA clades do not play a role in HA reassortment dynamics

Even though reassortment between AIVs is common in nature, emergence of stable reassorted IAV lineages is less common (25). Extensive investigation indicates that most reassortment events create unfit progeny virus, that is outcompeted by the wild-type virus (45). My data supports this, as all reassortant viruses displayed decreased replicative fitness compared to the wild-type virus, in MDCK-2 cells (Fig. 5). The lowered fitness of the reassortants is due to segment mismatch, where heterologous viral components are incompatible after reassortment (25).

Segment mismatch could be a result of RNA mismatch, where fewer RNA:RNA interactions between the heterologous vRNA segments results in inefficient packaging of the vRNA segments into a virion (25). If the lowered replicative fitness of the chicken H9N2(HA) reassortants are due to RNA mismatch, we would expect reassortants encoding an HA subtype in the same HA clade as H9 to exhibit higher fitness. However, the exact opposite was observed (Fig. 5). To support this, some HA subtypes from different HA clades exhibited similar replicative fitness and the H9N2(H10) reassortant (with an HA subtype from a different HA clade and group) displayed the highest replicative fitness of the HA reassortants (Fig. 5). In conclusion, there was no correlation between HA reassortant replicative fitness and their respective HA clade. This would suggest that RNA mismatch does not play a major role in the reassortment dynamics of HA subtypes. Support for this can be found in a recent study, showing that vRNA segments form a dynamic and redundant network of RNA:RNA interactions, across the whole vRNA segment (46). They found that influenza viruses have developed a balanced system to selectively package a full set of vRNA segments, while also accommodating heterologous vRNA segments, to promote reassortment.

Therefore, I suggest that protein mismatch should be investigated further, in order to understand the major factors governing HA subtype reassortment dynamics (25). There is an extensive amount of literature concerning the functional balance that is required between HA and NA segments (reviewed in 45). Different HA segments would have different affinities for the host cell receptor and hence their accompanying NA segment would match their activity (26). It has also been shown that mutations after reassortment restores the functional balance between HA and NA (48). To investigate whether the replicative fitness of HA subtype reassortants is dictated by the functional balance between HA and NA, one could generate more HA, NA and HA/NA reassortants of the chicken H9N2 AIV. Next, one could assess whether the fitter reassortants exhibit a balance in receptor binding affinity and receptor destruction activity, independently of the HA/NA subtype.

However, the replication kinetics experiment has several limitations. Firstly, the replicative fitness of the chicken H9N2(HA) reassortants in MDCK-2 cells does not reflect their evolutionary fitness in chickens. Alternatively, one could perform replication kinetics in DF-1 fibroblasts from chickens, to better replicate the conditions in live chickens. However, additional experimental studies in live chickens would ultimately be required, to support these findings. Important factors like transmissibility, tissue tropism, immune recognition and cross-

immunity in chickens are not accounted for here. Interestingly, a study found that heterosubtypic immunity to different HA subtypes in wild birds followed HA relatedness at the HA clade and group level (49). This would imply that distantly related HA subtypes might display even higher fitness advantages in live chickens, due to enhanced immune escape. This could also imply that HA reassortants could outcompete the wild-type virus, if the host has immunity against the wild-type HA subtype. Secondly, the virus concentrations were normalised by viral RNA copies. A more robust way to assess the replicative fitness of the HA reassortants would be to normalise the viruses by plaque forming units / ml. Thirdly, only one HA segment per HA subtype (except H9) were cloned. More HA segments from the same HA subtype should be tested, to assess whether the replicative fitness of an HA reassortant is consistent within the HA subtype.

Conclusion

Due to frequently causing asymptomatic infection in chickens, the H9N2 AIV has spread silently in poultry globally and become a panzootic in just under 30 years, causing a major threat to the economy and global health. In this time the virus has infected humans, exhibited evidence of mammalian adaptation and given rise to multiple AIV reassortants with enhanced zoonotic potential (8, 13, 15, 20, 22–24). Consequently, the H9N2 AIV deserves extensive research and global surveillance efforts, to prevent future zoonotic outbreaks and potentially a pandemic. Here, I report that the cDNA sequence of a variety of HA subtypes induces extensive recombination in *E. coli*, impeding efficient rescue of influenza viruses. Moreover, my data demonstrates that a poultry adapted H9N2 AIV isolated from chickens is compatible with at least ten HA subtypes from wild bird AIVs. This highlights the importance of reducing the spread of the virus in poultry, to reduce reassortment opportunities between H9N2 and other AIVs. However, all HA reassortants of the chicken H9N2 AIV displayed decreased replicative fitness in MDCK-2 cells, likely due to segment mismatch. Interestingly, the HA subtypes clustered into distinct HA clades and groups based on their phylogenetic relatedness. However, the HA clades did not correlate with the replicative fitness of the HA reassortants. This study explores the HA reassortment dynamics of poultry adapted H9N2 AIV *in vitro* and sets a framework for future experimental studies in live chickens. In order to be prepared for future zoonotic and poultry outbreaks of H9N2 AIV, it is imperative to understand the reassortment dynamics of H9N2.

ACKNOWLEDGEMENTS

Firstly, I am tremendously grateful for the daily supervision and academic guidance given by my main supervisor, Mahmoud Naguib, who has immensely enhanced my academic development. I also highly appreciate the guidance and feedback from my co-supervisor, Patrik Ellström. Next, I am grateful for the support with technical challenges and many fruitful discussions, from Anishia Wasberg and Julia Bergholm. I also thank Maria Rincon Gracia for support with technical challenges. In addition, I appreciate the assistance in cloning the H6 subtype, by Emma Brodin and Klara Martinovic. Lastly, I thank Åke Lundkvist for the opportunity to carry out the project at the Zoonosis Science Centre and all the help and support I have received from my colleagues here.

REFERENCES

1. Taubenberger JK, Morens DM. Pandemic influenza - including a risk assessment of H5N1: -EN- Pandemic influenza - including a risk assessment of H5N1 -FR- Les pandémies de grippe et l'évaluation du risque associé au sous-type H5N1 du virus de l'influenza -ES- Pandemias de influenza y evaluacíon de riegos del subtipo H5N1 del virus. Rev Sci Tech OIE [Internet]. 2009 Apr 1 [cited 2021 Mar 24];28(1):187–202. Available from: https://doc.oie.int/dyn/portal/index.seam?page=alo&aloId=30911

2. Johnson NPAS, Mueller J. Updating the Accounts: Global Mortality of the 1918-1920 "Spanish"; Influenza Pandemic. Bulletin of the History of Medicine [Internet]. 2002 [cited 2021 Mar 24];76(1):105–15. Available from: http://muse.jhu.edu/content/crossref/journals/bulletin_of_the_history_of_medicine/v076/76.1johnson.html

3. Somes MP, Turner RM, Dwyer LJ, Newall AT. Estimating the annual attack rate of seasonal influenza among unvaccinated individuals: A systematic review and meta-analysis. Vaccine [Internet]. 2018 May [cited 2021 Mar 24];36(23):3199–207. Available from: https://linkinghub.elsevier.com/retrieve/pii/S0264410X18305607

4. Paget J, Spreeuwenberg P, Charu V, Taylor RJ, Iuliano AD, Bresee J, et al. Global mortality associated with seasonal influenza epidemics: New burden estimates and predictors from the GLaMOR Project. Journal of Global Health [Internet]. 2019 Dec [cited 2021 Mar 24];9(2):020421. Available from: http://jogh.org/documents/issue201902/jogh-09-020421.pdf

5. Peteranderl C, Herold S, Schmoldt C. Human Influenza Virus Infections. Semin Respir Crit Care Med [Internet]. 2016 Aug 3 [cited 2021 Mar 24];37(04):487–500. Available from: http://www.thieme-connect.de/DOI/DOI?10.1055/s-0036-1584801

6. Dou D, Revol R, Östbye H, Wang H, Daniels R. Influenza A Virus Cell Entry, Replication, Virion Assembly and Movement. Front Immunol [Internet]. 2018 Jul 20 [cited 2021 Mar 24];9:1581. Available from: https://www.frontiersin.org/article/10.3389/fimmu.2018.01581/full

7. Taubenberger JK, Kash, John C. Influenza Virus Evolution, Host Adaptation, and Pandemic Formation. 2010;12.

8. Alexander DJ. An overview of the epidemiology of avian influenza. Vaccine [Internet]. 2007 Jul [cited 2021 Mar 24];25(30):5637–44. Available from: https://linkinghub.elsevier.com/retrieve/pii/S0264410X0601187X

9. Dugan VG, Chen R, Spiro DJ, Sengamalay N, Zaborsky J, Ghedin E, et al. The Evolutionary Genetics and Emergence of Avian Influenza Viruses in Wild Birds. Perez DR, editor. PLoS Pathog [Internet]. 2008 May 30 [cited 2021 Mar 25];4(5):e1000076. Available from: https://dx.plos.org/10.1371/journal.ppat.1000076

10. Wille M, Tolf C, Avril A, Latorre-Margalef N, Wallerström S, Olsen B, et al. Frequency and patterns of reassortment in natural influenza A virus infection in a reservoir host. Virology [Internet]. 2013 Aug [cited 2021 Mar 24];443(1):150–60. Available from: https://linkinghub.elsevier.com/retrieve/pii/S0042682213002638

11. Karl G Nicholson, John M Wood, Maria Zambon. Influenza. The Lancet [Internet]. 2003 [cited 2021 Mar 26]; Available from: https://www.thelancet.com/journals/lancet/article/PIIS0140-6736(03)14854-4/fulltext

12. Webster RG, William J. Bean, Owen T. Gorman, Chamers T, Kawaoka Y. Evolution and Ecology of Influenza A Viruses.pdf. 1992;

13. Mostafa A, Abdelwhab E, Mettenleiter T, Pleschka S. Zoonotic Potential of Influenza A Viruses: A Comprehensive Overview. Viruses [Internet]. 2018 Sep 13 [cited 2020 Oct 17];10(9):497. Available from: http://www.mdpi.com/1999-4915/10/9/497

14. Chmielewski R, Swayne DE. Avian Influenza: Public Health and Food Safety Concerns. Annu Rev Food Sci Technol [Internet]. 2011 Apr 10 [cited 2021 Mar 28];2(1):37–57. Available from: http://www.annualreviews.org/doi/10.1146/annurev-food-022510-133710

15. Peacock TP, James J, Sealy JE, Iqbal M. A Global Perspective on H9N2 Avian Influenza Virus. Viruses [Internet]. 2019 Jul 5 [cited 2020 Oct 17];11(7):620. Available from: https://www.mdpi.com/1999-4915/11/7/620

16. WHO. Cumulative number of confirmed human cases for avian influenza A(H5N1) reported to WHO, 2003-2020 [Internet]. WHO; 2020 [cited 2021 Mar 28]. Available from: https://www.who.int/influenza/human_animal_interface/H5N1_cumulative_table_archives/en/

17. Lin YP, Shaw M, Gregory V, Cameron K, Lim W, Klimov A, et al. Avian-to-human transmission of H9N2 subtype influenza A viruses: Relationship between H9N2 and H5N1 human isolates. Proceedings of the National Academy of Sciences [Internet]. 2000 Aug 15 [cited 2021 Mar 28];97(17):9654–8. Available from: http://www.pnas.org/cgi/doi/10.1073/pnas.160270697

18. Guan Y, Shortridge KF, Krauss S, Webster RG. Molecular characterization of H9N2 influenza viruses: Were they the donors of the 'internal' genes of H5N1 viruses in Hong Kong? Proceedings of the National Academy of Sciences [Internet]. 1999 Aug 3 [cited 2021 Mar 28];96(16):9363–7. Available from: http://www.pnas.org/cgi/doi/10.1073/pnas.96.16.9363

19. Pusch E, Suarez D. The Multifaceted Zoonotic Risk of H9N2 Avian Influenza. Veterinary Sciences [Internet]. 2018 Sep 21 [cited 2021 Mar 24];5(4):82. Available from: http://www.mdpi.com/2306-7381/5/4/82

20. Carnaccini S, Perez DR. H9 Influenza Viruses: An Emerging Challenge. Cold Spring Harb Perspect Med [Internet]. 2020 Jun [cited 2021 Mar 24];10(6):a038588. Available from: http://perspectivesinmedicine.cshlp.org/lookup/doi/10.1101/cshperspect.a038588

21. Khan SU, Anderson BD, Heil GL, Liang S, Gray GC. A Systematic Review and Meta-Analysis of the Seroprevalence of Influenza A(H9N2) Infection Among Humans. J Infect Dis [Internet]. 2015 Aug 15 [cited 2021 Apr 3];212(4):562–9. Available from: https://academic.oup.com/jid/article-lookup/doi/10.1093/infdis/jiv109

22. Song W, Qin K. Human-infecting influenza A (H9N2) virus: A forgotten potential pandemic strain? Zoonoses Public Health [Internet]. 2020 May [cited 2021 Mar 24];67(3):203–12. Available from: https://onlinelibrary.wiley.com/doi/abs/10.1111/zph.12685

23. Arai Y, Kawashita N, Ibrahim MS, Elgendy EM, Daidoji T, Ono T, et al. PB2 mutations arising during H9N2 influenza evolution in the Middle East confer enhanced replication and growth in mammals. Lauring AS, editor. PLoS Pathog [Internet]. 2019 Jul 2 [cited 2021 Mar 24];15(7):e1007919. Available from: https://dx.plos.org/10.1371/journal.ppat.1007919

24. Gu M, Xu L, Wang X, Liu X. Current situation of H9N2 subtype avian influenza in China. Vet Res [Internet]. 2017 Dec [cited 2021 Mar 24];48(1):49. Available from: http://veterinaryresearch.biomedcentral.com/articles/10.1186/s13567-017-0453-2

25. White MC, Lowen AC. Implications of segment mismatch for influenza A virus evolution. Journal of General Virology [Internet]. 2018 Jan 1 [cited 2020 Oct 17];99(1):3–16. Available from: https://www.microbiologyresearch.org/content/journal/jgv/10.1099/jgv.0.000989

26. Gaymard A, Le Briand N, Frobert E, Lina B, Escuret V. Functional balance between neuraminidase and haemagglutinin in influenza viruses. Clinical Microbiology and Infection [Internet]. 2016 Dec [cited 2021 Apr 4];22(12):975–83. Available from: https://linkinghub.elsevier.com/retrieve/pii/S1198743X16302312

27. Latorre-Margalef N, Tolf C, Grosbois V, Avril A, Bengtsson D, Wille M, et al. Long-term variation in influenza A virus prevalence and subtype diversity in migratory mallards in northern Europe. Proc R Soc B [Internet]. 2014 Apr 22 [cited 2021 Apr 5];281(1781):20140098. Available from: https://royalsocietypublishing.org/doi/10.1098/rspb.2014.0098

28. Chernomor O, von Haeseler A, Minh BQ. Terrace Aware Data Structure for Phylogenomic Inference from Supermatrices. Syst Biol [Internet]. 2016 Nov [cited 2021 Apr 11];65(6):997–1008. Available from: https://academic.oup.com/sysbio/article-lookup/doi/10.1093/sysbio/syw037

29. Letunic I, Bork P. Interactive Tree Of Life (iTOL) v4: recent updates and new developments. Nucleic Acids Research [Internet]. 2019 Jul 2 [cited 2021 Apr 11];47(W1):W256–9. Available from: https://academic.oup.com/nar/article/47/W1/W256/5424068

30. Bacterial Transformation Protocol [Internet]. Addgene. [cited 2021 Apr 5]. Available from: https://www.addgene.org/protocols/bacterial-transformation/

31. Mostafa A, Kanrai P, Ziebuhr J, Pleschka S. Improved dual promotor-driven reverse genetics system for influenza viruses. Journal of Virological Methods [Internet]. 2013 Nov [cited 2021 Mar 24];193(2):603–10. Available from: https://linkinghub.elsevier.com/retrieve/pii/S0166093413002759

32. Brauer R, Chen P. Influenza Virus Propagation in Embryonated Chicken Eggs. JoVE [Internet]. 2015 Mar 19 [cited 2021 Mar 24];(97):52421. Available from:

http://www.jove.com/video/52421/influenza-virus-propagation-in-embryonated-chicken-eggs

33. World Organisation for Animal Health. OIE Terrestrial Manual 2018 [Internet]. 2018. Available from: https://www.oie.int/standard-setting/terrestrial-manual/

34. Hierholzer JC, Killington RA. Virus isolation and quantitation. Virology Methods Manual [Internet]. 1996 [cited 2021 May 3];25–46. Available from: https://www.ncbi.nlm.nih.gov/pmc/articles/PMC7173433/

35. Hadley Wickham, Winston Chang, Lionel Henry, Thomas Lin Pedersen, Kohske Takahashi, Claus Wilke, Kara Woo, Hiroaki Yutani, Dewey Dunnington. ggplot2 - plugin RStudio [Internet]. [cited 2021 May 22]. Available from: https://ggplot2.tidyverse.org/

36. Hoffmann E, Neumann G, Kawaoka Y, Hobom G, Webster RG. A DNA transfection system for generation of influenza A virus from eight plasmids. Proceedings of the National Academy of Sciences [Internet]. 2000 May 23 [cited 2020 Oct 18];97(11):6108–13. Available from: http://www.pnas.org/cgi/doi/10.1073/pnas.100133697

37. Mostafa A, Kanrai P, Petersen H, Ibrahim S, Rautenschlein S, Pleschka S. Efficient Generation of Recombinant Influenza A Viruses Employing a New Approach to Overcome the Genetic Instability of HA Segments. Krammer F, editor. PLoS ONE [Internet]. 2015 Jan 23 [cited 2021 Mar 24];10(1):e0116917. Available from: https://dx.plos.org/10.1371/journal.pone.0116917

38. Zhou B, Jerzak G, Scholes DT, Donnelly ME, Li Y, Wentworth DE. Reverse genetics plasmid for cloning unstable Influenza A virus gene segments. Journal of Virological Methods [Internet]. 2011 May [cited 2021 Mar 24];173(2):378–83. Available from: https://linkinghub.elsevier.com/retrieve/pii/S0166093411000528

39. Bhat S, Bialy D, Sealy JE, Sadeyen J-R, Chang P, Iqbal M. A ligation and restriction enzyme independent cloning technique: an alternative to conventional methods for cloning hard-to-clone gene segments in the influenza reverse genetics system. Virol J [Internet]. 2020 Dec [cited 2021 May 8];17(1):82. Available from: https://virologyj.biomedcentral.com/articles/10.1186/s12985-020-01358-2

40. Lewin A, Mayer M, Chusainow J, Jacob D, Appel B. Viral promoters can initiate expression of toxin genes introduced into Escherichia coli. BMC Biotechnol [Internet]. 2005 [cited 2021 May 7];5(1):19. Available from: http://bmcbiotechnol.biomedcentral.com/articles/10.1186/1472-6750-5-19

41. Lu L, Lycett SJ, Leigh Brown AJ. Reassortment patterns of avian influenza virus internal segments among different subtypes. BMC Evol Biol [Internet]. 2014 [cited 2021 Mar 24];14(1):16. Available from: http://bmcevolbiol.biomedcentral.com/articles/10.1186/1471-2148-14-16

42. Munster VJ, Baas C, Lexmond P, Waldenström J, Wallensten A, Fransson T, et al. Spatial, Temporal, and Species Variation in Prevalence of Influenza A Viruses in Wild

Migratory Birds. Kawaoka Y, editor. PLoS Pathog [Internet]. 2007 May 11 [cited 2021 May 19];3(5):e61. Available from: https://dx.plos.org/10.1371/journal.ppat.0030061

43. Keawcharoen J, Spronken MIJ, Vuong O, Bestebroer TM, Munster VJ, Osterhaus ADME, et al. Repository of Eurasian influenza A virus hemagglutinin and neuraminidase reverse genetics vectors and recombinant viruses. Vaccine [Internet]. 2010 Aug [cited 2021 Mar 24];28(36):5803–9. Available from: https://linkinghub.elsevier.com/retrieve/pii/S0264410X1000900X

44. Lam TT-Y, Wang J, Shen Y, Zhou B, Duan L, Cheung C-L, et al. The genesis and source of the H7N9 influenza viruses causing human infections in China. Nature [Internet]. 2013 Oct [cited 2021 May 22];502(7470):241–4. Available from: http://www.nature.com/articles/nature12515

45. Villa M, Lässig M. Fitness cost of reassortment in human influenza. Wilke CO, editor. PLoS Pathog [Internet]. 2017 Nov 7 [cited 2021 May 19];13(11):e1006685. Available from: https://dx.plos.org/10.1371/journal.ppat.1006685

46. Dadonaite B, Gilbertson B, Knight ML, Trifkovic S, Rockman S, Laederach A, et al. The structure of the influenza A virus genome. Nat Microbiol [Internet]. 2019 Nov [cited 2021 Apr 4];4(11):1781–9. Available from: http://www.nature.com/articles/s41564-019-0513-7

47. de Vries E, Du W, Guo H, de Haan CAM. Influenza A Virus Hemagglutinin–Neuraminidase–Receptor Balance: Preserving Virus Motility. Trends in Microbiology [Internet]. 2020 Jan [cited 2021 Apr 4];28(1):57–67. Available from: https://linkinghub.elsevier.com/retrieve/pii/S0966842X19302355

48. Kaverin NV, Gambaryan AS, Bovin NV, Rudneva IA, Shilov AA, Khodova OM, et al. Postreassortment Changes in Influenza A Virus Hemagglutinin Restoring HA–NA Functional Match. Virology [Internet]. 1998 May [cited 2021 May 20];244(2):315–21. Available from: https://linkinghub.elsevier.com/retrieve/pii/S004268229899119X

49. Latorre-Margalef N, Grosbois V, Wahlgren J, Munster VJ, Tolf C, Fouchier RAM, et al. Heterosubtypic Immunity to Influenza A Virus Infections in Mallards May Explain Existence of Multiple Virus Subtypes. Ferguson N, editor. PLoS Pathog [Internet]. 2013 Jun 20 [cited 2021 Mar 24];9(6):e1003443. Available from: https://dx.plos.org/10.1371/journal.ppat.1003443